

1 **Electronic Supplementary Information**

2

3 **Development of a Hydrophilic Interaction Liquid Chromatography (HILIC) Method for the**
4 **Chemical Characterization of Water-Soluble Isoprene Epoxydiol (IEPOX)-Derived**
5 **Secondary Organic Aerosol**

6 Tianqu Cui^{1,a}, Zhexi Zeng^{1,a}, Erickson O. dos Santos², Zhenfa Zhang¹, Yuzhi Chen¹, Yue Zhang^{1,3},
7 Caitlin A. Rose¹, Sri H. Budisulistiorini^{1,b}, Leonard B. Collins¹, Wanda M. Bodnar¹, Rodrigo A.
8 F. de Souza⁴, Scot T. Martin^{5,6}, Cristine M. D. Machado², Barbara J. Turpin¹, Avram Gold¹,
9 Andrew P. Ault^{7,8}, Jason D. Surratt^{1,*}

10 ¹ Department of Environmental Sciences and Engineering, Gillings School of Global Public
11 Health, The University of North Carolina at Chapel Hill, Chapel Hill, North Carolina, USA

12 ² Department of Chemistry, Federal University of Amazonas, Manaus, Amazonas, Brazil

13 ³ Aerodyne Research Inc., Billerica, Massachusetts, USA

14 ⁴ Superior School of Technology, University of the State of Amazonas, Manaus, Amazonas, Brazil

15 ⁵ School of Engineering and Applied Sciences, Harvard University, Cambridge, Massachusetts,
16 USA

17 ⁶ Department of Earth and Planetary Sciences, Harvard University, Cambridge, Massachusetts,
18 USA

19 ⁷ Department of Environmental Health Sciences, University of Michigan, Ann Arbor, Michigan,
20 USA

21 ⁸ Department of Chemistry, University of Michigan, Ann Arbor, Michigan, USA

22

23

24 ^a These authors contributed equally to the work presented here.

25 ^b Current address: Earth Observatory of Singapore, Nanyang Technological University, Singapore

26

27

28 *To whom correspondence should be addressed.

29 Tel: (919)-966-0470. Fax: (919)-966-7911. Email: surratt@unc.edu (J.D.S.)

30

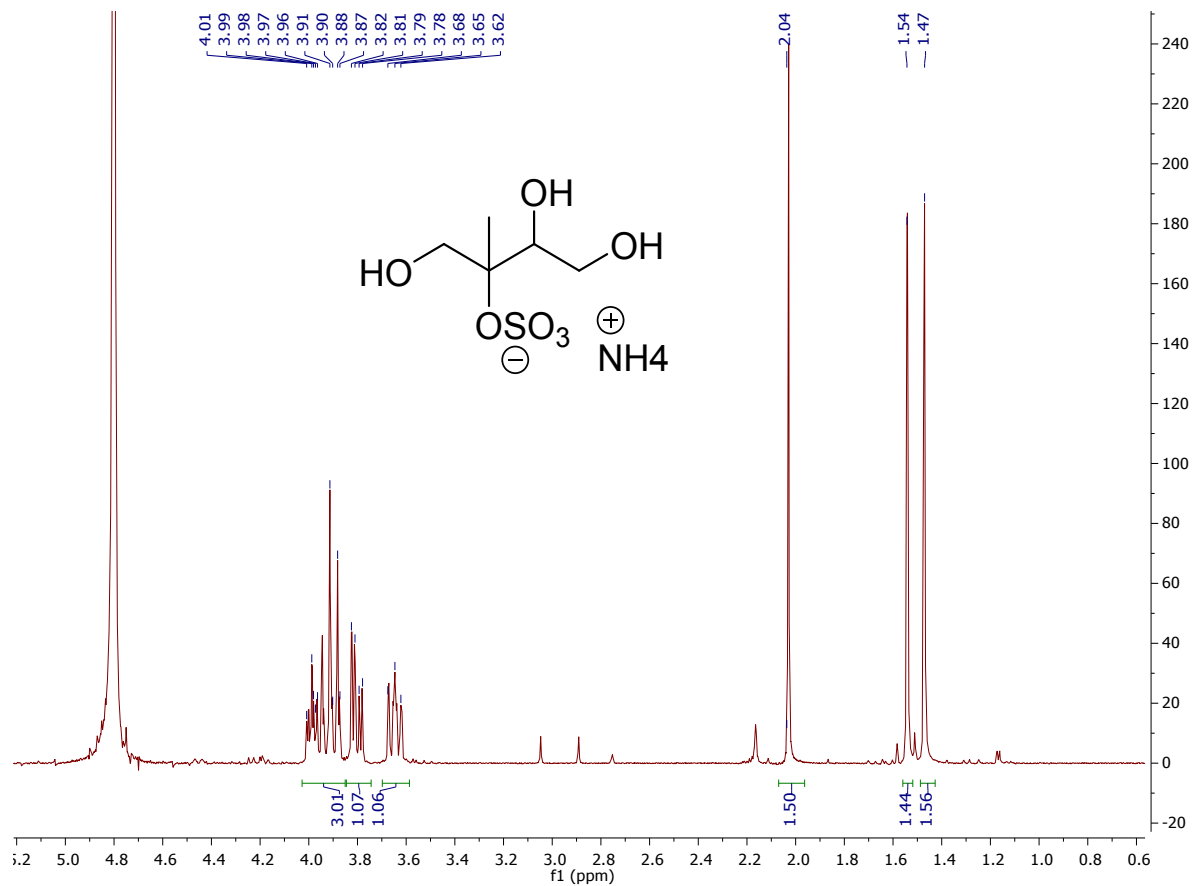
31

32

33

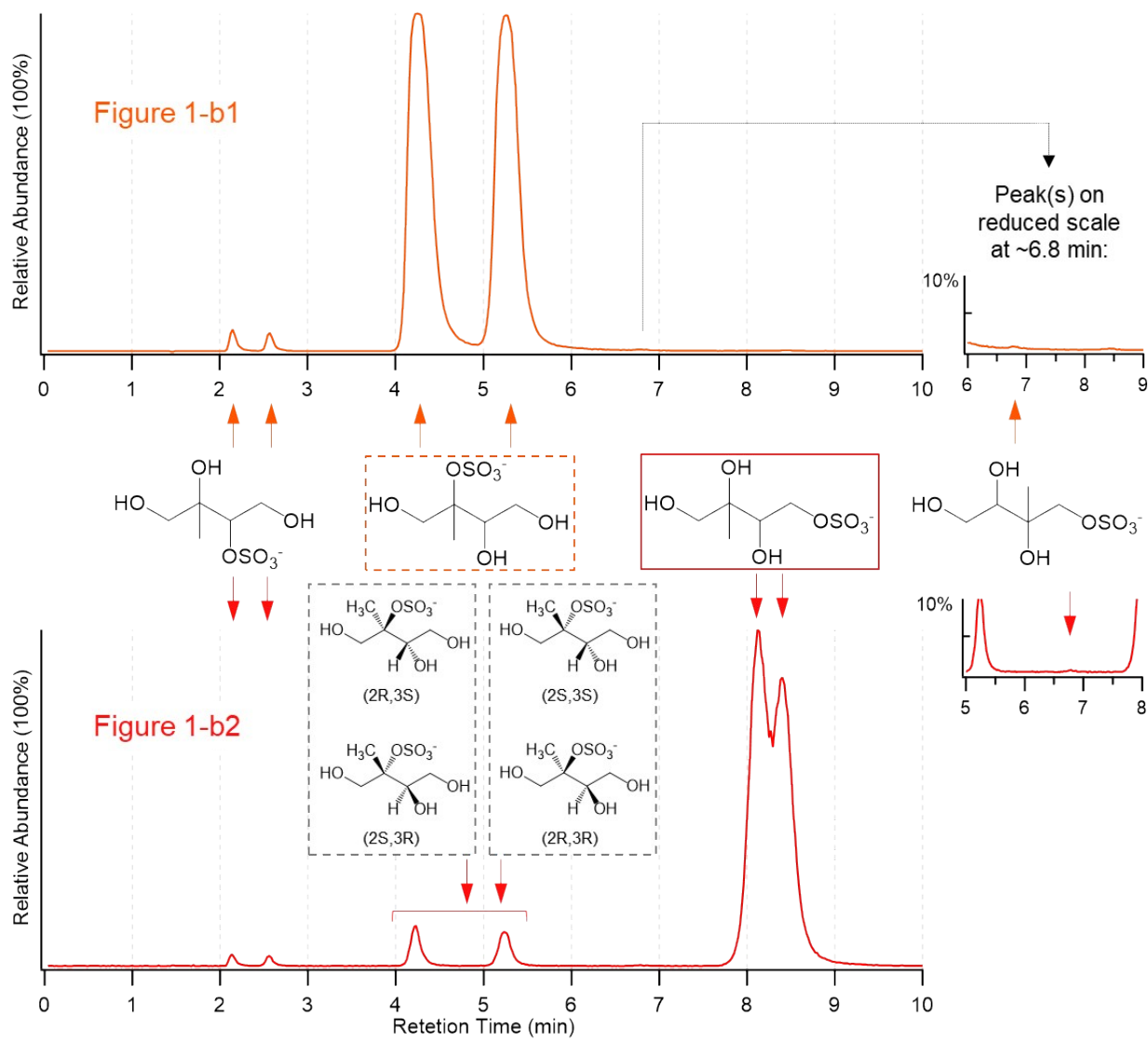
34 For Submission to: Environmental Science: Processes & Impacts

35



36

37 **Figure S1.** Structure and ¹H NMR (D₂O, 400 MHz) of 2-methyltetrol sulfate diastereomer standard
 38 (ammonium 1, 3, 4-trihydroxy-2-methylbutan-2-yl sulfate; optical configurations indicated below
 39 in Figure S2).

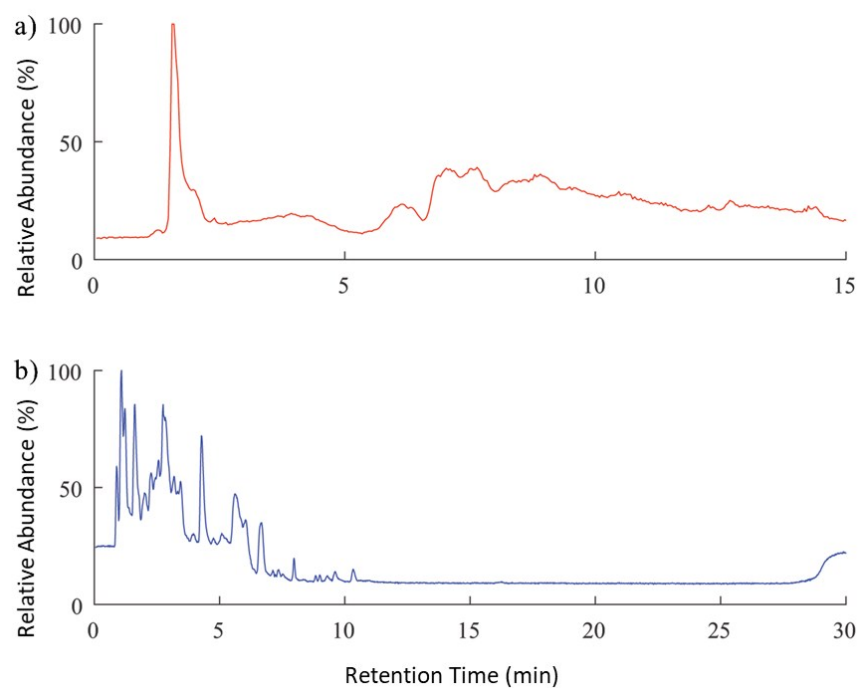


40

41 **Figure S2.** The EICs in Figure 1 (b1-b2) are reproduced here for the 2- and 3-methyltetrol sulfate
 42 standards. The tertiary methyltetrol sulfate esters with correct optical configurations at the
 43 asymmetric centers are enclosed in dashed grey boxes. The top row of structures shows all possible
 44 the structural isomers without optical configurations indicated. From left to right: 1,3,4-trihydroxy-
 45 3-methylbutan-2-yl sulfate, 1,3,4-trihydroxy-2-methylbutan-2-yl sulfate (2-methyltetrol sulfate, in
 46 dashed orange box), 2,3,4-trihydroxy-3-methylbutyl sulfate (3-methyltetrol sulfate in solid red
 47 box), and 2,3,4-trihydroxy-2-methylbutyl sulfate. In the insets at the right side of the figure, EICs
 48 at a reduced scale (10%) indicate a trace peak(s) at ~6.8 min, which may represent the primary
 49 sulfate ester derived from δ -IEPOX (2,3,4-trihydroxy-2-methylbutyl sulfate).

50

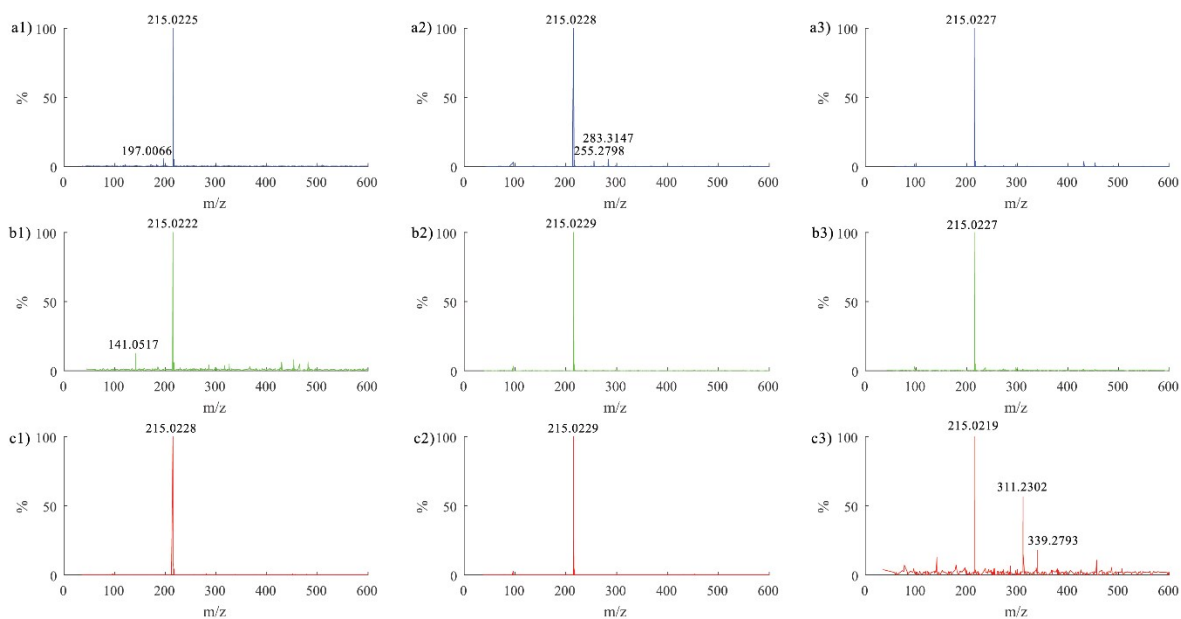
51



52

53 **Figure S3.** Total ion chromatograms (TICs) of a laboratory-generated β -IEPOX-derived SOA
54 sample separated on **a)** RPLC C_{18} column, and **b)** HILIC BEH amide column.

55



56

57 **Figure S4.** Mass spectra from HILIC/ESI-HR-QTOFMS of the chromatographic peak of *m/z*
 58 215.023 from **a)** 10 $\mu\text{g mL}^{-1}$ standard of 3-methyltetrol sulfate, **b)** laboratory-generated δ -IEPOX
 59 SOA, and **c)** PM_{2.5} sample collected at Look Rock during 2013 SOAS campaign, at RT at: 1) 2.2
 60 min; 2) 4.5 min; and 3) 9.6 min. Note that the chromatographic peak in “c3” has significantly
 61 smaller response rate compared to the other chromatographic peaks.

63 **Aerosol Volume Measurement, Mass Calculation, and Mass Closure for Laboratory-**
64 **Generated SOA**

65 Chamber aerosol number distributions, which were subsequently converted to total aerosol
66 surface area and volume concentrations, were measured by a scanning electrical mobility system
67 (SEMS v5.0, Brechtel Manufacturing Inc. – BMI) containing a differential mobility analyzer
68 (DMA, BMI) coupled to a mixing condensation particle counter (MCPC Model 1710, BMI). The
69 SEMS system has an internal Nafion dryer connected inline between its inlet and neutralizer. Total
70 aerosol mass concentration was calculated using the total volume concentration multiplied by the
71 density of 1.42 g mL⁻¹ of the particles formed after reaction (for the seed aerosol of acidified
72 ammonium sulfate, a density of 1.77 g mL⁻¹ was used). The densities used above were reported
73 by Riva et al. based on single-particle characterizations from experiments conducted with *trans*-
74 β-IEPOX and acidified ammonium sulfate aerosols under similar conditions.¹ However, the
75 volume growth was found to be lower for δ-IEPOX-derived SOA, which means the resulting
76 density was higher than 1.42 g mL⁻¹. Therefore, assuming the widely reported organic density of
77 1.2 g mL⁻¹ and volume additivity, the resulting density for total aerosol has been corrected to 1.55
78 g mL⁻¹, which was used to calculate the mass of total aerosols generated from δ-IEPOX and
79 acidified ammonium sulfate. It is also reasonable to assume that sulfates, either in inorganic or
80 organic forms, remained in the aerosol phase and the change in ammonium equilibrium between
81 the gas and aerosol phase after IEPOX uptake was small as indicated by Aerosol Chemical
82 Speciation Monitor (ACSM, Aerodyne Research Inc.) measurements. Therefore, the calculated
83 aerosol mass concentration includes both the inorganic sulfate group and the sulfate groups that
84 are covalently bonded to the organic residue. The averaged aerosol masses during the PILS
85 collection periods for the two chamber experiments are shown in Table S1 below.

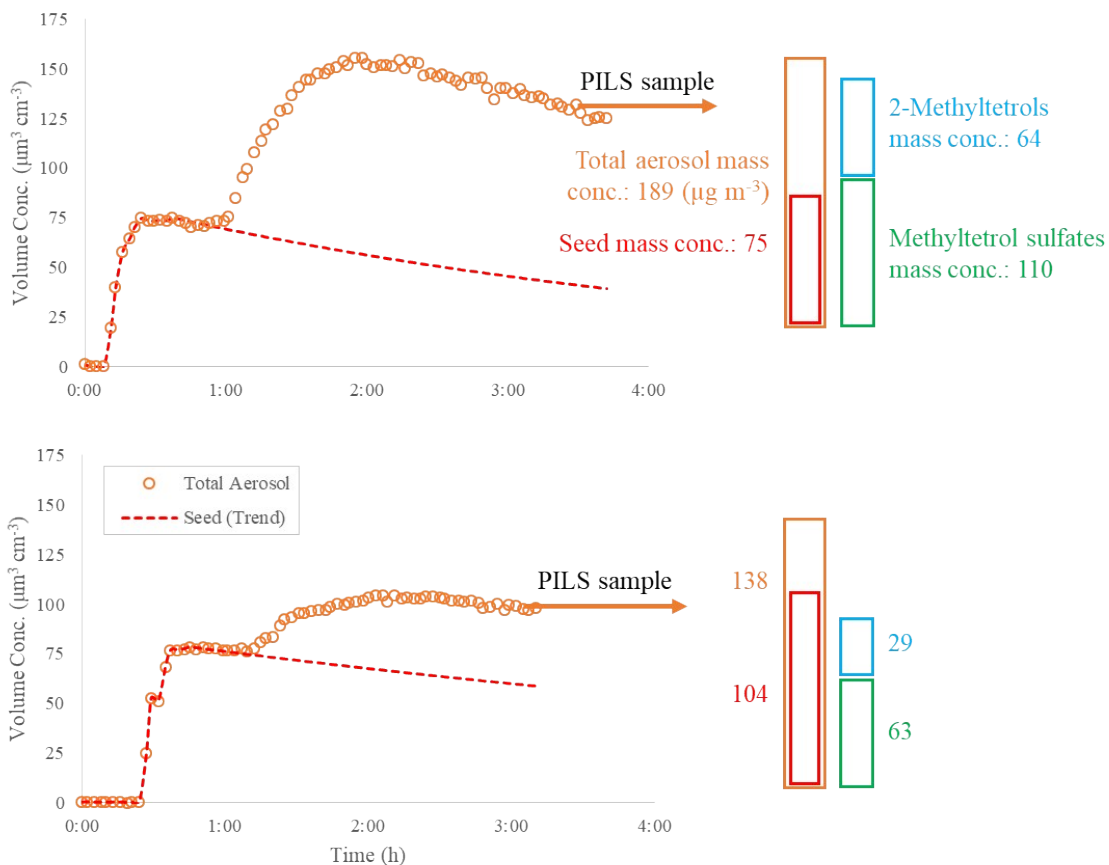
86 **Table S1.** Experimental Conditions and Calculated Aerosol Mass for Laboratory-Generated
87 IEPOX SOA

IEPOX Isomer	Seed Aerosols	Aerosol Mass ($\mu\text{g m}^{-3}$)	Temp ($^{\circ}\text{C}$)	RH (%)
<i>trans</i> - β -IEPOX	$(\text{NH}_4)_2\text{SO}_4 + \text{H}_2\text{SO}_4$	188.51	21-23	50-50
δ -IEPOX	$(\text{NH}_4)_2\text{SO}_4 + \text{H}_2\text{SO}_4$	150.13	21-23	50-55

88

89 Figure S5 shows the aerosol volume concentration and the seed volume decay during the
90 experiments. For the laboratory-generated SOA from *trans*- β -IEPOX (top), the PILS sample
91 selected was collected near the end of the experiment at time 3:27 with 2-methyltetrols measured
92 to be $\sim 64 \mu\text{g m}^{-3}$ and methyltetrol sulfates measured to be $\sim 110 \mu\text{g m}^{-3}$. At the same time, the
93 SEMS-MCPC system measured $133 \mu\text{m}^3 \text{cm}^{-3}$ total particle volume concentration, which was
94 converted to a total mass concentration of $189 \mu\text{g m}^{-3}$ (density = 1.42 g mL^{-1}); and $42 \mu\text{m}^3 \text{cm}^{-3}$
95 seed particle volume concentration (assuming first-order decay rate), which was converted to a
96 total seed mass concentration of $75 \mu\text{g m}^{-3}$ (density = 1.77 g mL^{-1}). Thus, the two quantified
97 IEPOX SOA components accounted for $\sim 92\%$ of the total aerosol mass, which suggests that the
98 inorganic sulfate in the seed aerosol might be substantially converted into organosulfates. This was
99 supported by measurements using ion chromatography for the PILS samples collected during the
100 course of the experiment. These details are being expanded upon in another manuscript just
101 submitted. A similar mass-closure situation was observed for the laboratory-generated SOA from
102 δ -IEPOX (Figure S5, bottom).

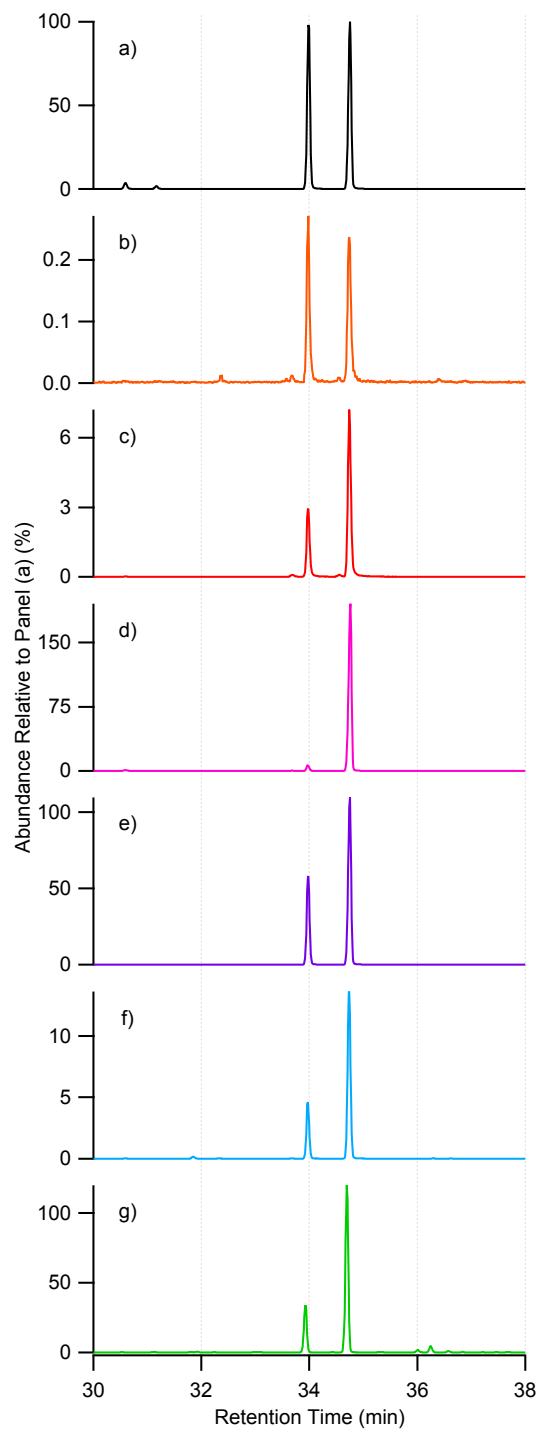
103



104

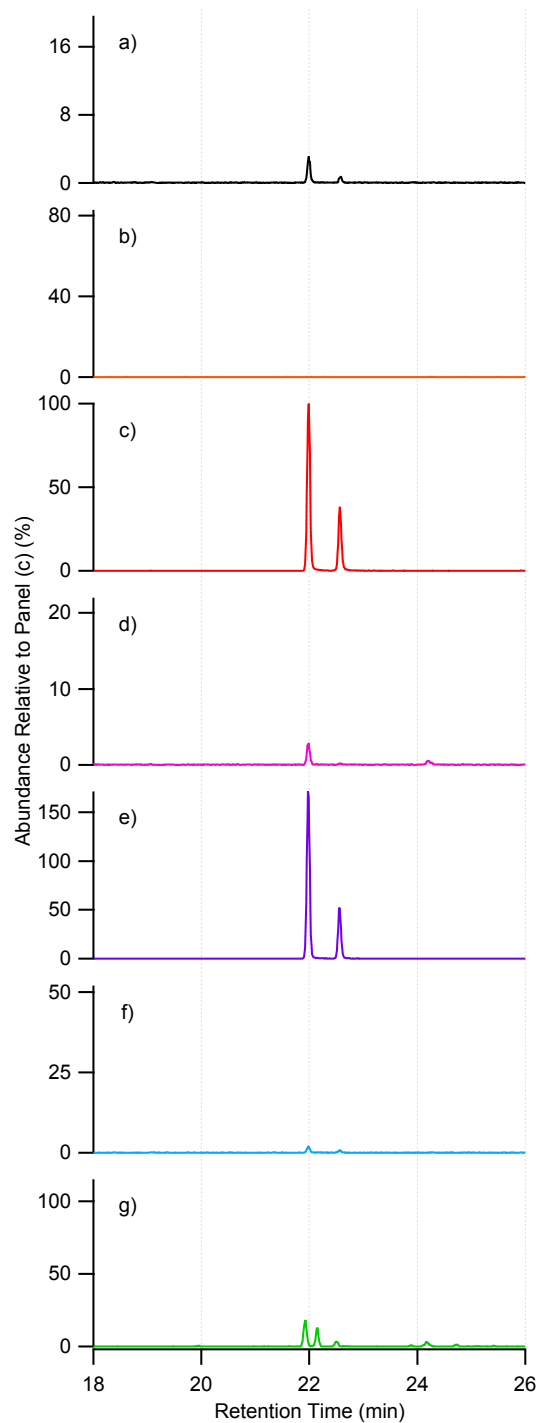
105 **Figure S5.** Time profile of total aerosol volume concentration and aerosol mass breakdown for
 106 the experiments from (top) *trans*- β -IEPOX; and (bottom) δ -IEPOX. Ammonium bisulfate particles
 107 were injected into the chamber to reach $\sim 75 \mu\text{m}^3 \text{cm}^{-3}$. After seed injection, the chamber was left
 108 static for at least 30 min to ensure that the seed aerosol was stable and uniformly mixed. Then, 30
 109 mg of *trans*- β - or δ -IEPOX was injected into the chamber. PILS collection was performed at the
 110 end of each experiment, as indicated by the arrow. The bars on the right side show the mass
 111 concentrations of the total particles, the initial seed particles measured by the SEMS. 2-
 112 Methyltetrols and methyltetrol sulfates concentrations were measured by the HILIC/ESI-HR-
 113 QTOFMS protocol and indicated by the blue and green bars as well.

114



115

116 **Figure S6.** GC/EI-MS EICs of m/z 219 corresponding to 2-methyltetrols (RT = 34.0, 34.8 min)
 117 from: **a)** $50 \mu\text{g mL}^{-1}$ standard of 2-methyltetrol; **b)** $50 \mu\text{g mL}^{-1}$ standard of 2-methyltetrol sulfate;
 118 **c)** $50 \mu\text{g mL}^{-1}$ standard of 3-methyltetrol sulfate; **d)** laboratory-generated β -IEPOX SOA; **e)**
 119 laboratory-generated δ -IEPOX SOA; **f)** $\text{PM}_{2.5}$ sample at Look Rock during 2013 SOAS campaign;
 120 **g)** $\text{PM}_{2.5}$ sample at Manaus in Nov. 2016. Note that the y-axis scale was adjusted to the highest
 121 peak in each panel, with the labelled abundance in percentage relative to that in Panel (a).



122

123 **Figure S7.** GC/EI-MS EICs of m/z 262 corresponding to 3-MeTHF-3,4-diols (RT = 22.0, 22.6
 124 min) from: **a)** $50 \mu\text{g mL}^{-1}$ standard of 2-methyltetrol; **b)** $50 \mu\text{g mL}^{-1}$ standard of 2-methyltetrol
 125 sulfate; **c)** $50 \mu\text{g mL}^{-1}$ standard of 3-methyltetrol sulfate; **d)** laboratory-generated β -IEPOX SOA;
 126 **e)** laboratory-generated δ -IEPOX SOA; **f)** $\text{PM}_{2.5}$ sample at Look Rock during 2013 SOAS
 127 campaign; **g)** $\text{PM}_{2.5}$ sample at Manaus in Nov. 2016. Note that the y-axis scale was adjusted to the
 128 highest peak in each panel, with the labelled abundance in percentage relative to that in Panel (c).

129 **Estimation of C₅-Alkene Triols, 2-Methyltetrols, and 3-MeTHF-3,4-diols Potentially**
130 **Resulting from Thermal Degradation of Methyltetrol Sulfates**

131 As shown in Figure 5, a large amount of C₅-alkene triols was observed from the 2-
132 methyltetrol sulfate standard using GC/EI-MS, while 2-methyltetrols (Figure S6) and 3-MeTHF-
133 3,4-diols (Figure S7) were observed from the 3-methyltetrol sulfate standard. By running both
134 methyltetrol sulfate standards from 0.25-50 µg mL⁻¹, we established a semi-quantitative
135 relationship between the response of C₅-alkene triols (as well as 2-methyltetrols and 3-MeTHF-
136 3,4-diols) produced and the concentrations of 2- (or 3-) methyltetrol sulfate standards prepared.
137 For example, the response factor of C₅-alkene triols was determined to be 15301 peak area (in EIC
138 of *m/z* 231 at 26.9, 27.9, and 28.3 min, see Figure 5) per 1 µg mL⁻¹ of 2-methyltetrol sulfate
139 standard. In Table S2, 2-methyltetrol sulfate from the laboratory-generated SOA from β-IEPOX
140 was measured using HILIC/ESI-HR-QTOFMS to be 1.773 µg mL⁻¹ in the 150 µL of solution after
141 reconstitution. The solvent of reconstitution was 95:5 ACN/water for HILIC/ESI-HR-QTOFMS
142 or 2:1 BSTFA (N,O-bis (trimethylsilyl) trifluoroacetamide + trimethylchlorosilane, 99:1, Supelco)
143 /pyridine for GC/EI-MS. After correction for the 200-fold dilution, 2-methyltetrol sulfate was
144 determined to be 355 µg mL⁻¹ as listed in the table. In another aliquot of the same filter extract,
145 the response of C₅-alkene triols was back-calculated as a result of 1183 µg mL⁻¹ 2-methyltetrol
146 sulfate, according to the semi-quantitative relationship described above, assuming the same yield
147 of C₅-alkene triols from the 2-methyltetrol sulfate standard, since the standards and samples were
148 analyzed in one GC/EI-MS sequence.

149 By doing this, as shown in Table S2, we attribute 30.0% (355 µg mL⁻¹/1183 µg mL⁻¹ =
150 30.0%), 42.8%, and 14.7% of the C₅-alkene triols to the potential thermal degradation of 2-

151 methyltetrol sulfate from the laboratory-generated SOA from β -IEPOX, the Look Rock, and the
 152 Manaus samples, respectively.

153 **Table S2.** Estimation of C₅-Alkene Triols due to Thermal Degradation of 2-Methyltetrol Sulfate

	2-Methyltetrol sulfate measured	C ₅ -Alkene triols attributed to 2-methyltetrol sulfate	
	$\mu\text{g mL}^{-1}$	$\mu\text{g mL}^{-1}$	%
Lab. SOA from β -IEPOX	355 ^a	1183	30.0%
Look Rock, TN, USA	58	136	42.8%
Manaus, Brazil	175	1185	14.7%

154 ^a The concentrations are converted to those in the 150- μL solution after reconstitution for the dried filter extract.

155

156 Similarly, the response factors of 2-methyltetrols and 3-MeTHF-3,4-diols were determined
 157 to be 5659 and 2169 peak area per 1 $\mu\text{g mL}^{-1}$ of 3-methyltetrol sulfate standard, respectively. Thus,
 158 as shown in Table S3, thermal degradation of 3-methyltetrol sulfate might result in 11.1% and over
 159 100% (112.3%) of the 2-methyltetrols and 3-MeTHF-3,4-diols observed in the laboratory-
 160 generated SOA from δ -IEPOX.

161

162 **Table S3.** Estimation of 2-Methyltetrols and 3-MeTHF-3,4-diols due to Thermal Degradation of
 163 3-Methyltetrol Sulfate

	3-Methyltetrol sulfate measured	2-Methyltetrols attributed to 3-methyltetrol sulfate		3-MeTHF-3,4-diols attributed to 3-methyltetrol sulfate	
	$\mu\text{g mL}^{-1}$	$\mu\text{g mL}^{-1}$	%	$\mu\text{g mL}^{-1}$	%
Lab. SOA from δ -IEPOX	361 ^a	3247	11.1%	322	112.3%

164 ^a The concentrations are converted to those in the 150- μL solution after reconstitution for the dried filter extracts.

165

166

167

168 **Reference**

- 169 (1) Riva, M.; Bell, D. M.; Hansen, A.-M.; Drozd, G. T.; Zhang, Z.; Gold, A.; Imre, D.; Surratt, J.
170 D.; Glasius, M.; Zelenyuk, A. Effect of Organic Coatings, Humidity and Aerosol Acidity on
171 Multiphase Chemistry of Isoprene Epoxydiols. *Environ. Sci. Technol.*, 2016, 5580–8, 50 (11).
- 172 (2) A. P. S. Hettiyadura, T. Jayarathne, K. Baumann, A. H. Goldstein, J. A. de Gouw, A. Koss, F.
173 N. Keutsch, K. Skog, and E. A. Stone, Qualitative and quantitative analysis of atmospheric
174 organosulfates in Centreville, Alabama, *Atmos. Chem. Phys.*, 2017, 17, 1343–1359.